Interaction of two point vortices with an external wave: Application to plasma drift waves

Xavier Leoncini, Alberto Verga

Interaction of two point vortices with an external wave: Application to plasma drift waves

Xavier Leoncini*
Aix-Marseille Université, CPT-CNRS UMR 6207,
Campus de Luminy, Case 907 - 13288 Marseille cedex 9, France

Alberto Verga†
Aix-Marseille Université, IM2NP-CNRS UMR 6242,
Campus de St Jérôme, Case 142, 13397 Marseille, France
(Dated: February 7, 2011)

The complex interactions of concentrated vortices with self-generated waves is investigated using a model of point vortices in the presence of an external wave. In spite of its simplicity, this model shows a rich dynamical behavior including oscillations of a dipole, splitting and merging of two like-circulation vortices, and chaos. The analytical and numerical results of this model have been found to predict under certain conditions, the behavior of more complex systems, such as the vortices of the Charney-Hasegawa-Mima equation (drift waves or geostrophic flows), where the presence of waves strongly affects the evolution of large coherent structures.

PACS numbers: 47.32.Cc,52.35.Kt

I. INTRODUCTION

Physical systems like large scale motion in oceans and atmospheres [1–3], space and laboratory plasmas [4, 5], or in statistical physics, the XY planar spin model [6, 7], are all able to generate both vortices and waves, whose interaction is one of the keys to their behavior. The phenomenology of these systems is very rich, ranging from turbulence to self-organization, formation of coherent structures [8–10] and anomalous transport [11–13]. Understanding the elementary mechanisms dominating the dynamics is crucial to model the statistical properties of these flows. One important fundamental process is the vortex interaction in presence of waves. Indeed, it has been observed that collisions of vortices may induce their merging, and on the other hand, the inverse process of splitting is also possible, large vortices may break under the action of waves. Both mechanisms are accompanied by the emission of waves, as for instance in the interaction of plasma vortices and drift waves [14–16].

The role played by waves in the interaction and evolution of vortices is not well known. A comparison of the long-time evolution of Euler decaying two-dimensional turbulence [10] and the Hasegawa-Mima one (which supports wave modes) [17], shows that the relaxation towards a kind of thermodynamic equilibrium state [18] is much longer or unreachable in presence of a wave field [19–21]. This illustrates that vortex interactions are largely influenced by the presence of waves.

A common feature of these vortex-wave systems is that they are almost two-dimensional and may be described by a conservation equation which is a slight generalization of the vorticity Euler equation. In general the existence of vortex solutions is related to the so-called Poisson nonlinearity, which is the two-dimensional version of the convective nonlinearity in a normal fluid, or the electrostatic drift in magnetized plasmas. Besides, waves may be related to some source of divergence of the velocity field, as compressibility or as in the two-dimensional reduction of a layered flow. The equation for the generalized vorticity Ω, containing these basic mechanisms (a linear dispersion relation, and a Poisson nonlinearity) is given by

$$\frac{\partial \Omega}{\partial t} + [\Omega, \psi] = 0 \,, \tag{1}$$

where $[\cdot,\cdot]$ is the usual Poisson bracket, and ψ is the stream function; the actual relation $\Omega = F(\psi)$ depends on the considered physical system, for the Euler equation it is simply given by $\Omega = -\nabla^2\psi$. This equation expresses the conservation of the generalized vorticity following the current lines. The Hasegawa-Mima equation for plasma drift waves, also known in fluid mechanics as the geostrophic equation for Rossby waves [4, 22, 23], reduces to (1) with the generalized vorticity,

$$\Omega = -\nabla^2\psi + \psi/\rho_s^2 - (v_d/\rho_s^2)\, x \,, \tag{2}$$

where ψ is, in this context, related to the electric potential (in suitable units) in the plasma, ρ_s is the hybrid Larmor radius and v_d is the drift wave velocity. The similarity of the equations governing Rossby waves in the atmosphere and drift waves in a plasma, may be traced back to the analogy between Coriolis and Lorentz forces, which determine the form of the dispersion relation, and the common convective nonlinearity, which reduces to a Poisson bracket in two dimensions. The two parameters, a length scale and characteristic velocity, are related to important physical effects which modify the system evo-

*Xavier.Leoncini@cpt.univ-mrs.fr
†Alberto.Verga@univ-provence.fr

lution with respect to the simpler Euler fluid. The Larmor radius is a characteristic length which introduces a finite range interaction between concentrated vortices. The drift velocity is related to the phase velocity of drift waves, the dispersion relation being

$$\omega_{\boldsymbol{k}} = v_d k_y/(1+\rho_s^2 k^2)\,, \tag{3}$$

with ω the frequency and $\boldsymbol{k}$ the two-dimensional wavenumber. The Hasegawa-Mima equation admits both localized vortex and wave solutions [16, 24], allowing a rich nonlinear dynamics as shown in numerical simulations.

The vortex-wave interaction is in general extremely complicated, involving the emision and scattering of waves by the vortices and simultaneously the deformation of the vortex shape by the wave field. Although the wave term in (2), proportional to the x-coordinate, is obviously non localized and it forbids the solution of the Hasegawa-Mima equation (1) in the form of an assembly of point vortices [25], in a first approximation we may consider a system where the vorticity is highly concentreted but subject to the action of a wave field in such a way that the effect of the vortices on the wave may be neglected. Therefore, we propose a simple model of point vortices, implying that the velocity field is almost everywhere potential, in the externally imposed field of a single wave. This model, which is amenable to an analytical treatement, may serve to investigate the wave-vortex interaction in the context of equations of the form of (1). In this case the vortex structure becomes trivial and the feedback on the wave is neglected. The velocity field may be written as a superposition of two terms, one related to the point vortices and one related to the wave. We show that processes such as propagation, splitting and fusion of vortices, which involve the binary collision of localized structures, may be modeled by a system of two point vortices under the action of an external wave.

In the following section we state the basic equations of the point vortex model. In Sec. III we investigate the different dynamical regimes that the presence of the wave can induce in the motion of the point vortices, we describe the dipole (opposite circulation vortices) and the monopole (like-circulation vortices) trajectories, we find the range of parameters where the strong interaction of the monopole and the wave leads to their merging or splitting. In Sec. IV we compare the results of Sec. III with numerical simulations of the Hasegawa-Mima equation, and finally (Sec. V) we conclude with a summary and brief discussion of the results.

II. POINT VORTEX MODEL

Point vortices are known to be exact solutions of Euler equations [26], that is when the vorticity is given by $\Omega = -\nabla^2\psi$, but they also are exact solutions of the more general equation (1), when $\Omega = -\nabla^2\psi + \psi/\rho_s^2$. In the second case the usual logarithmic interaction is replaced by a modified Bessel function K_0 interaction. Point vortices are defined by a vorticity distribution given by a superposition of Dirac functions,

$$\Omega(\boldsymbol{x},t) = \frac{1}{2\pi}\sum_{\alpha=1}^{N}\Gamma_\alpha\delta\left(\boldsymbol{x}-\boldsymbol{x}_\alpha(t)\right)\,, \tag{4}$$

where $\boldsymbol{x}$ is a vector in the plane of the flow, Γ_α is the circulation of vortex α, N is the total number of vortices, and $\boldsymbol{x}_\alpha(t)$ is the vortex position at time t. Using this expression of the vorticity and solving the Poisson equation, in the Euler case, or the Helmholtz equation in the more general case, one obtains the current function associated to the point vortices. By Helmholtz theorem [27], the motion of the vortices is determined by the value of the velocity field at the position of the vortex. If the velocity field is written as $\boldsymbol{v} = \boldsymbol{e}_z \wedge \nabla\psi + \nabla\phi$, where $\boldsymbol{e}_z$ is the unit vector perpendicular to the plane of the flow, and ϕ takes into account the potential flow, in general the point vortex motion is

$$\Gamma_\alpha\dot{\boldsymbol{x}}_\alpha = \boldsymbol{e}_z \wedge \frac{\partial H}{\partial \boldsymbol{x}_\alpha} + \Gamma_\alpha\nabla\phi\,. \tag{5}$$

where the Hamiltonian H is given by

$$H = \frac{1}{2\pi}\sum_{\alpha>\beta}\Gamma_\alpha\Gamma_\beta U(|\boldsymbol{x}_\alpha - \boldsymbol{x}_\beta|) \tag{6}$$

with $U(x) = -\log(x)$ in the Euler case, and $U(x) = \mathrm{K}_0(x/\rho_s)$ in the more general case (when $\rho_s \to \infty$ the modified Bessel function tends to the logarithm). When the distance between the vortices is smaller than the typical interaction length (ρ_s) the behavior of the two systems is similar, in the opposite case, the K_0 interaction decrease exponentially and the vortices are almost free. In the following, analytical computations will be made using the simpler logarithmic interaction, generalization to the modified Bessel interaction is straightforward. The basic equations of the model are directly derived from (5), where the wave potential is simply defined by $\phi = \Gamma_0\cos(\boldsymbol{k}\cdot\boldsymbol{x} - \omega t)$, with Γ_0 the wave amplitude, $\boldsymbol{k}$ the wave vector, and ω is the wave pulsation,

$$\dot{\boldsymbol{r}} = \Gamma_+\boldsymbol{e}_z \wedge \frac{\boldsymbol{r}}{r^2} - 2\Gamma_0\boldsymbol{k}\cos\left(\boldsymbol{k}\cdot\boldsymbol{R} - \omega t\right)\sin\left(\frac{\boldsymbol{k}\cdot\boldsymbol{r}}{2}\right)\,, \tag{7}$$

$$\dot{\boldsymbol{R}} = \Gamma_-\boldsymbol{e}_z \wedge \frac{\boldsymbol{r}}{2r^2} - \Gamma_0\boldsymbol{k}\sin\left(\boldsymbol{k}\cdot\boldsymbol{R} - \omega t\right)\cos\left(\frac{\boldsymbol{k}\cdot\boldsymbol{r}}{2}\right)\,, \tag{8}$$

where $\boldsymbol{r} = \boldsymbol{r}_1 - \boldsymbol{r}_2$ is the relative postion of the vortices, $\boldsymbol{R} = (\boldsymbol{r}_1 + \boldsymbol{r}_2)/2$ is their "center of mass", and $\Gamma_+ = (\Gamma_1 + \Gamma_2)/2\pi$, $\Gamma_- = (\Gamma_1 - \Gamma_2)/2\pi$, are their reduced circulations.

For further calculations, it is useful to measure the lengths in $1/k$ and the time in $1/\omega$, and to perform a Galileo transformation to the frame moving at the wave phase velocity, which leads to the following nondimensional variables and parameters: $x' = \boldsymbol{k}\cdot\boldsymbol{r}/2$,

$y' = \boldsymbol{k}\cdot(\boldsymbol{e}_z\wedge\boldsymbol{r})/2$, $t' = \omega t$, $X' = \boldsymbol{k}\cdot\boldsymbol{R} - \tau$, $Y' = \boldsymbol{k}\cdot(\boldsymbol{e}_z\wedge\boldsymbol{R})$, and the new vectors $\boldsymbol{r} = (x', y')$, $\boldsymbol{R} = (X', Y')$ (in the following we drop the primes) and the parameters $\alpha_0 = \Gamma_0 k^2/\omega$, for the wave amplitude $\alpha_+ = \Gamma_+ k^2/4\omega$, $\alpha_- = \Gamma_- k^2/4\omega$, for the vortices circulation. The coordinate system is chosen, without loss of generality, so that the x-axis is parallel to the vector $\boldsymbol{k}$. The parameter α_0 measures the strength of the wave, and α_+, α_- are the effective vortex circulations.

Two cases are of special interest, the so called "dipole", when the vortices have opposite circulations $\alpha_+ = 0$, and the "monopole", when the vortices have the same circulation $\alpha_- = 0$. Without wave the dipole moves in a straight line, and the monopole follows a circular trajectory.

In the dipole case, the equations of motion reduces to the completely integrable system

$$\dot{x} = -\alpha_0 \cos X \sin x\,, \tag{9a}$$
$$\dot{y} = 0\,, \tag{9b}$$
$$\dot{X} = -1 - \alpha_0 \sin X \cos x + \alpha_- \frac{y}{r^2}\,, \tag{9c}$$
$$\dot{Y} = -\alpha_- \frac{x}{r^2}\,. \tag{9d}$$

where $r^2 = x^2 + y^2$.

In the monopole case it is convenient to introduce polar coordinates: $x = r\cos\theta$, $y = r\sin\theta$, to obtain the system,

$$\dot{r} = -\alpha_0 \cos X \sin(r\cos\theta)\cos\theta\,, \tag{10a}$$
$$r\dot{\theta} = \frac{\alpha_+}{r} + \alpha_0 \cos X \sin(r\cos\theta)\sin\theta\,, \tag{10b}$$
$$\dot{X} = -1 - \alpha_0 \sin X \cos(r\cos\theta)\,, \tag{10c}$$
$$\dot{Y} = 0\,. \tag{10d}$$

These three autonomous nonlinear equations allow chaotic behavior of the vortex trajectories, the external wave destroying the vortex integrals of motion. The systems (9) and (10) are the basic equations of our model.

III. DYNAMICS OF TWO POINT VORTICES IN THE FIELD OF A WAVE

In this section we study the motion of the point vortices for the two configurations, dipole and monopole, using analytical and numerical methods. The numerical analysis is performed by direct computation of the point vortices trajectories,

$$\dot{\boldsymbol{x}}_1 = g \begin{pmatrix} y_1 - y_2 \\ x_2 - x_1 \end{pmatrix} \frac{K_1(\nu r)}{r} - \hat{\boldsymbol{x}} a \sin(x_1 - t)\,, \tag{11a}$$
$$\dot{\boldsymbol{x}}_2 = \mp g \begin{pmatrix} y_2 - y_1 \\ x_1 - x_2 \end{pmatrix} \frac{K_1(\nu r)}{r} - \hat{\boldsymbol{x}} a \sin(x_2 - t)\,, \tag{11b}$$

for arbitrary $\nu = 1/k\rho_s$, or

$$\dot{\boldsymbol{x}}_1 = \frac{1}{r^2} \begin{pmatrix} y_1 - y_2 \\ x_2 - x_1 \end{pmatrix} - \hat{\boldsymbol{x}} \alpha_0 \sin(x_1 - t)\,, \tag{12a}$$
$$\dot{\boldsymbol{x}}_2 = \mp \frac{1}{r^2} \begin{pmatrix} y_2 - y_1 \\ x_1 - x_2 \end{pmatrix} - \hat{\boldsymbol{x}} \alpha_0 \sin(x_2 - t)\,, \tag{12b}$$

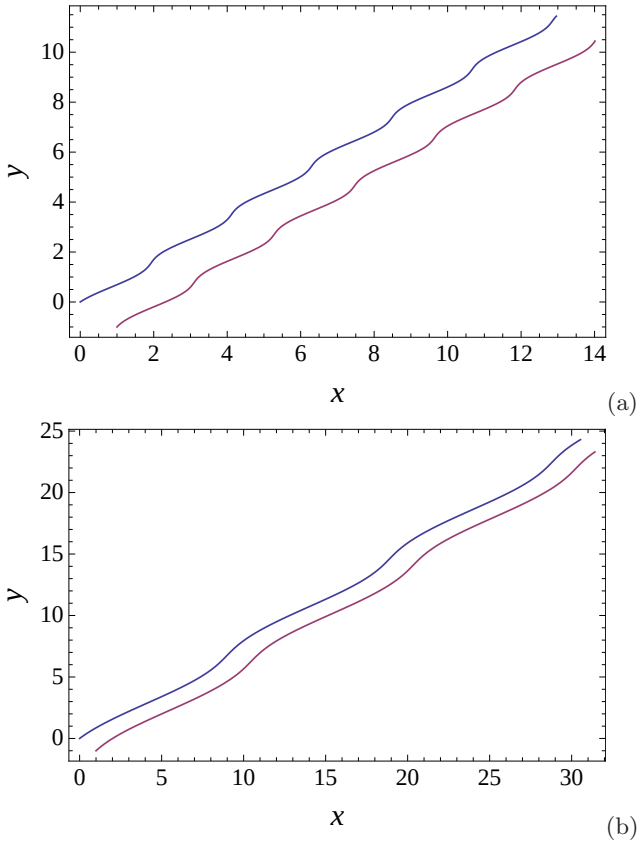

FIG. 1. (Color online) Trajectory of the dipole vortex with a weak wave. The initial conditions for the two point vortices and the wave are $\boldsymbol{x}_1 = (0, 0)$, $\boldsymbol{x}_2 = (1, -1)$, $t_f = 50\pi$, $g = 1$, $a = 0.3$, where t_f is the final time.

in the limit $\nu \to 0$. We used $g = k^2\Gamma/\omega k\rho_s$ ($\Gamma = \Gamma_1 = -\Gamma_2$ for the dipole, minus sign, and $\Gamma = \Gamma_1 = \Gamma_2$ for the monopole, plus sign, and $a = \alpha_0/k\rho_s$. Units are such that $k = 1$ and $\omega = 1$, with the vector $\boldsymbol{k}$ chosen parallel to the x-axis. Most numerical integrations of (11) were performed with $g = 1$ and $\nu = 1$, and varying the wave amplitude a and the initial distance between the vortices.

Let us start with the analysis of the dipole trajectories (see Fig. 1). As mentioned, the motion of a dipole interacting with a wave is integrable. The quadrature is difficult, but a first insight can be given by the study of particular exact solutions of the motion.

Solutions with $\boldsymbol{r} = \boldsymbol{r}_0$ constant exist if $x = n\pi$. We can then define $\omega_0 = \alpha_-/({r_0}^2)$, the characteristic frequency of the dipole, and $V = -1 + \omega_0 y_0$, the $x-$component of the speed of the unperturbed dipole in the frame of the wave. We obtain for $\boldsymbol{R}$

$$\dot{X} = V + (-1)^{n+1}\alpha_0 \sin X \qquad Y = -\omega_0 x_0 \tau\,. \tag{13}$$

This equation naturally leads to two different cases, depending on the value of $|V/\alpha_0|$, which determines the existence of a fixe point for X. In one case ($|V| > \alpha_0|$) the x-component of the dipole speed $\dot{X}$ maintains constant sign, while it is subject to a change of sign in the

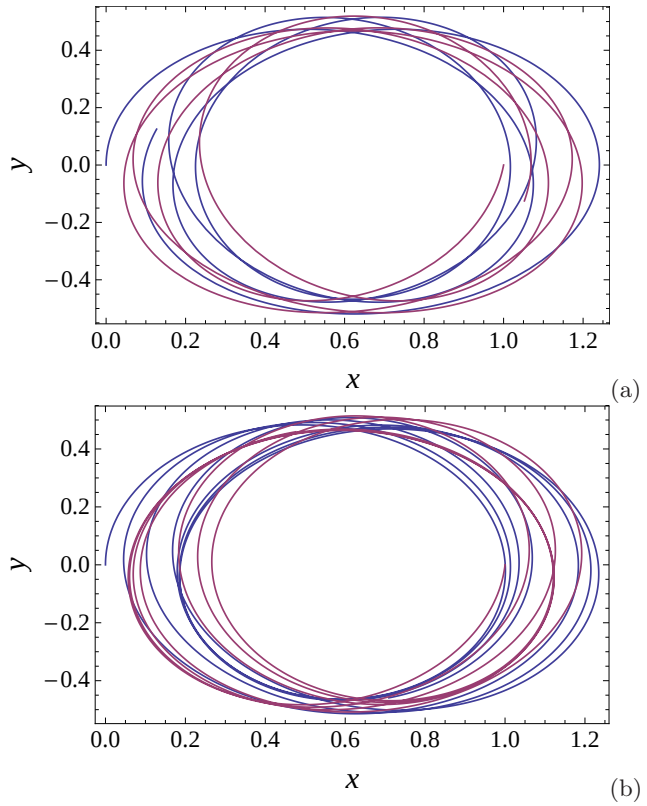

FIG. 2. (Color online) Trajectory of the monopole vortex with a weak wave. The initial conditions for the two point vortices and the wave are $\boldsymbol{x}_1 = (0,0)$, $\boldsymbol{x}_2 = (1,0)$, $t_f = 20$, $g = 1$, $a = 0.1$.

opposite case ($|V| < \alpha_0|$) and approach a fixed point.

We first notice, that in the very simple case where $V = 0$ (the x-component of speed of the unperturbed dipole is equal to the phase velocity), which we call the resonant case, the equation (13) becomes $\dot{X} = (-1)^{n+1}\alpha_0 \sin X$. This equation predicts the existence of selected directions $X = n\pi$ for the dipole propagation, a feature reminiscent to the mode locking phenomenon as for instance the one observed by in [28, 29]. These directions correspond to the case where the dipole is located at an extremum of the wave, and therefore where the profile of the wave is flat. Therefore, if the condition $V = 0$ is satisfied the dipole will only see this flat profile and the influence of the wave on the dipole motion vanishes. Indeed, the general solution of (13) for $V = 0$ is

$$X = 2\arctan\left(\tan\left(\frac{X_0}{2}\right)\exp\left((-1)^{n+1}\alpha_0\tau\right)\right) , \quad (14)$$

and the dipole sets itself in one of the selected directions where it does not see the wave.

An analog behavior is found when $|V/\alpha_0| < 1$, the solutions of (13), show that $X(\tau)$ is going to converge towards the following fixed value $X_f = (-1)^n \arcsin\left(\frac{V}{\alpha_0}\right) + m\pi$. The difference here is that the dipole is trapped , and the wave forces the x-component of the speed of the dipole to the phase velocity ω/k, by adjusting the slope of the wave that the dipole will "see".

On the other hand, if $|V/\alpha_0| > 1$, the dipole has enough strength to "surpass" the wave with V as the averaged x-component of its speed. The wave has only a small influence on the dipole. We remind that all the previous results are made without any assumption on the intensity of the wave α_0. This study of simple solutions let us guess that there might be, two types of dynamical regimes, one where the dipole is trapped, and therefore fixed points of the dynamics exist, the system is in a constant "dissipative" or "exciting" regime whether the dipole is accelerated or slowed to ω/k, and another one where the dipole "surpass" the wave, the system oscillates between dissipative and exciting regimes. This seems to be confirmed by the run of numerous simulations using a wide range of parameters values and initial conditions, and we can suspect that the presence of a wave is not going to affect much the structure of the dipole. Another way to convince ourselves with this affirmation is to perform a perturbative calculation to the fisrt order with a small wave. The development is then possible if we assume that $\alpha_0/V \ll 1$. It seems therefore that a weak wave ($\alpha_0 \ll \alpha_-$) will only affect the dipole near the resonance ($V = 0$), which is the exact situation where our particular solution do not "see" the wave. In Fig. 1 we can see the trajectory of the dipole in a weak wave field for the two cases, short and long range vortex interaction of Eqs. (11) and (12) respectively.

In the case of the "monopole" ($\alpha_- = 0$), the dynamics result in three coupled equations (10), which allow complex trajectories as is shown in the series of Figs. 2, 3, 4, 5 and 6. Therefore, in order to investigate this case, we make different perturbative approaches, which can qualitatively describe the behavior of the monopole in different physical situations. We first investigate the long wavelength behavior with a weak wave, then the long wave behavior itself, and finally we discuss the small wave length behavior. In the last two approaches, we particularly focus on the merging or splitting trajectories.

To perform the perturbative calculation in long-wave approximation with a weak wave, we assume that $|\alpha_0| \sim r \ll 1$, and $|\alpha_+| \sim 1$; the consistency of these assumption will be valid as long as r remain within the neighborhood of r_0. A series perturbation development gives then,

$$r = r_0 \qquad \theta = \omega_0\tau , \quad (15)$$

$$X = \tau - \alpha_0\cos\tau \qquad Y = Y_0 , \quad (16)$$

where $\omega_0 = \alpha_+/{r_0}^2$ is the natural frequency of the unperturbed monopole. The vortex trajectories are therefore confined in a small region of maximum thickness $2\alpha_0$ around the circle. A simulation of this situation can be seen in Fig. 2.

But if we only assume that $r \ll 1$ and $|\alpha_0| \sim |\alpha_+| \approx 1$ (the wave is not weak anymore), the motion equations

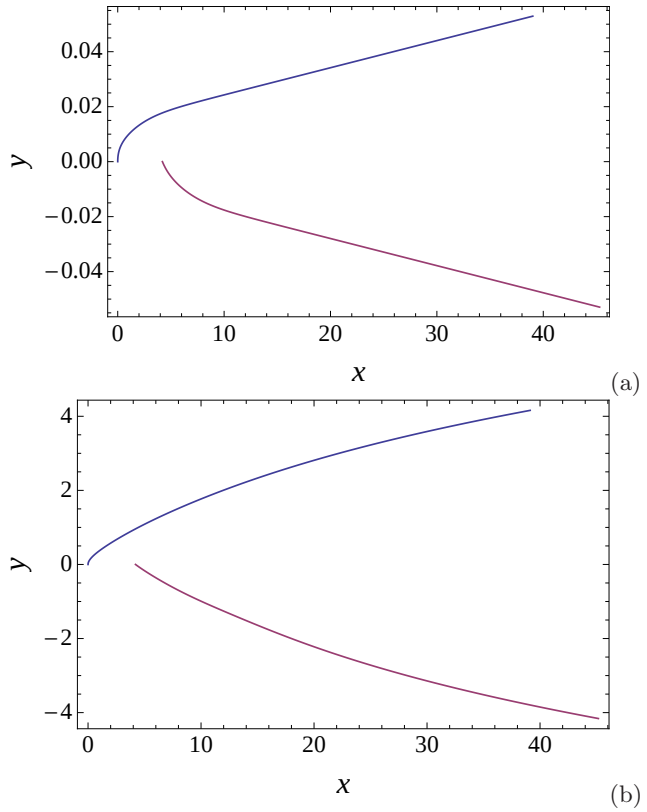

FIG. 3. (Color online) Trajectory of the monopole leading to the splitting. The initial conditions for the two point vortices and the wave are $\boldsymbol{x}_1 = (0,0)$, $\boldsymbol{x}_2 = (4.2,0)$, $t_f = 40$, $\Gamma_1 = 1$, $\Gamma_2 = 1$, $\Gamma_0 = 1.2$, $\omega = 1.$.

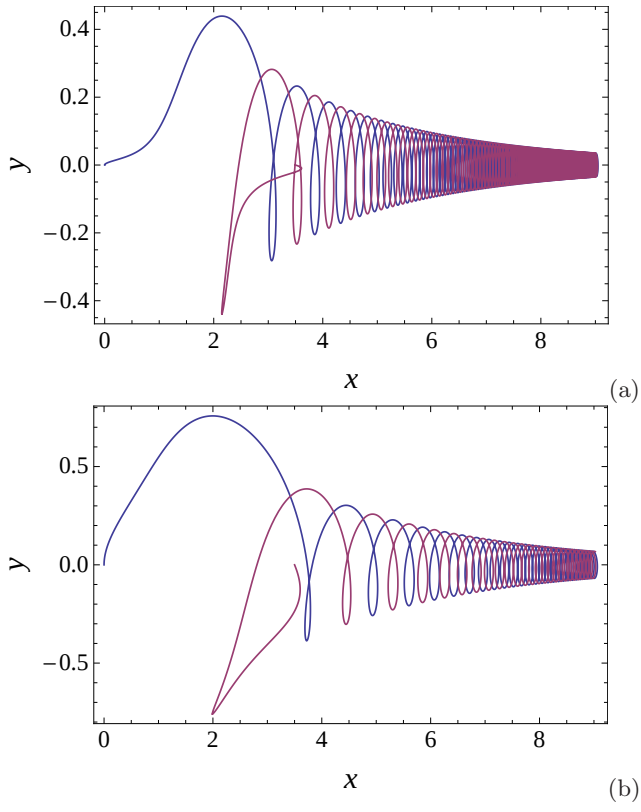

FIG. 4. (Color online) Trajectory of the monopole leading to the fusion. The initial conditions for the two point vortices and the wave are $\boldsymbol{x}_1 = (0,0)$, $\boldsymbol{x}_2 = (3.5,0)$, $t_f = 15$, $\Gamma_1 = 1$, $\Gamma_2 = 1$, $\Gamma_0 = 0.5$, $\omega = 1.$.

become,

$$\dot{\theta} = \frac{\alpha_+}{r^2}\,, \tag{17a}$$

$$\dot{r} = -\alpha_0 r\cos^2\theta\cos X \approx -\frac{\alpha_0}{2} r\cos X\,, \tag{17b}$$

$$\dot{X} = -1 - \alpha_0\sin X\,, \tag{17c}$$

where in the distance equation (17b), we approximated the cosine term by its mean value, using the fact that in the limit $r \to 0$, θ given by (17a) varies rapidly. We then obtain for X an equation similar to (13) with $V = 1$; it can be readily integrated to give

$$X(t) = -2\arctan\left[\alpha_0 + s\tan\left(\frac{s}{2}(t-t_0)\right)\right] \tag{18}$$

for $\alpha_0 < 1$, and for $\alpha_0 > 1$,

$$X(t) = -2\arctan\left[\alpha_0 - s\tanh\left(\frac{s}{2}(t-t_0)\right)\right]\,, \tag{19}$$

where $s = |\alpha_0^2 - 1|^{1/2}$. In the case where $\alpha_0 > 1$, X converges to a fixed value $X_f = -2\arctan(\alpha_0 - \sqrt{\alpha_0^2 - 1})$, given for the distance r the long-time solution,

$$r \to r_0 \exp\left[-\frac{\alpha_0}{2}\cos(X_f)t\right]\,, \tag{20}$$

where $\cos X_f$ is positive for $\alpha_0 > 1$. Therefore, we obtain in this case an exponential approach of the two vortices, accompanied with a diverging angular velocity $\dot{\theta} \to \infty$. The merging characteristic time is $2/\alpha_0\cos X_f(\alpha_0)$, and within the present approximation, it diverges when $\alpha_0 \to 1$. This is consistent with the vortex merging observed in the numerical solutions, as seen in Fig. 4.

In the other case, $\alpha_0 < 1$ and $r \ll 1$, quasi-periodic motion is possible. Indeed, $X(t)$ is periodic in t, with a period $2\pi/\sqrt{1-\alpha_0^2}$. In the weak wave amplitude limit, one retrieves the perturbation result, with $X(t) \approx X_0(t) = t(1-\alpha_0^2)/(1+\alpha_0^2) - 2\arctan(\alpha_0)$ linear and

$$r \approx r_0 \exp\left[-\frac{\alpha_0(1+\alpha_0^2)}{2(1-\alpha_0^2)}\sin X_0(t)\right]\,, \tag{21}$$

Let us now consider the situation where, $r \gg 1$ (the wave length is small compared to the size of the monopole), $1 \lesssim \alpha_0 \sim \alpha_+ \ll r$, such that the first term in (10b) may be neglected. Equations (10) become now,

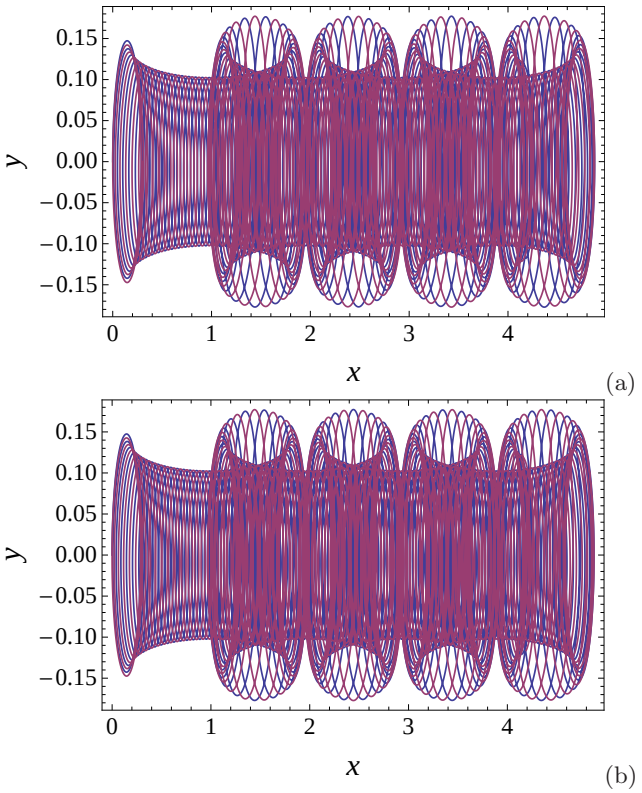

FIG. 5. (Color online) Quasi-periodic motion of the monopole. The initial conditions for the two point vortices and the wave are $\boldsymbol{r}_1 = (0,0)$, $\boldsymbol{r}_2 = (0.3,0)$, $t_f = 200$, $\Gamma_1 = 1$, $\Gamma_2 = 1$, $\Gamma_0 = 0.5$, $\omega = 1$.

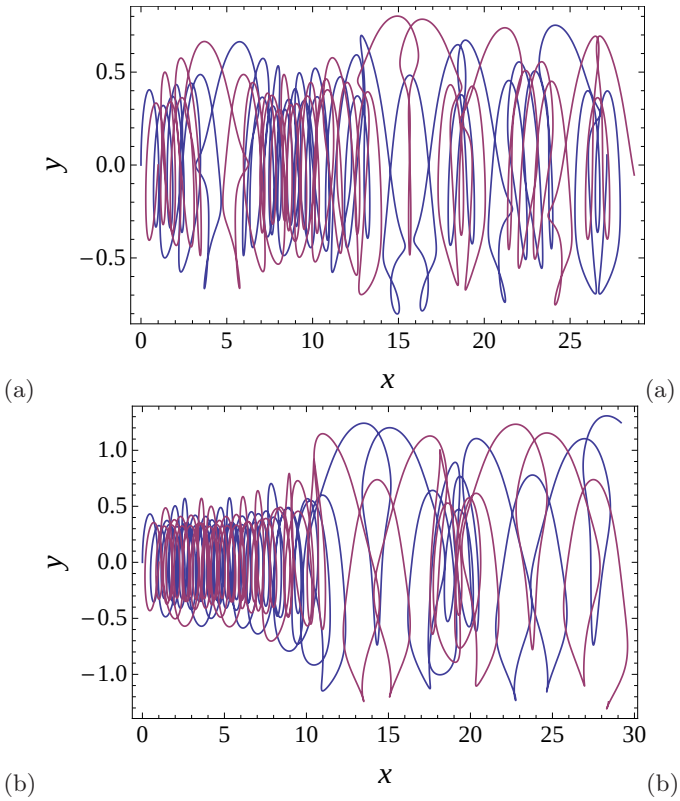

FIG. 6. (Color online) Complex trajectory of the monopole. The initial conditions for the two point vortices and the wave are $\boldsymbol{r}_1 = (0,0)$, $\boldsymbol{r}_2 = (1,0)$, $t_f = 200$, $\Gamma_1 = 1$, $\Gamma_2 = 1$, $\Gamma_0 = 0.5$, $\omega = 1$.

$\theta \approx$ const. and

$$\dot{x} = -\alpha_0 \cos X \sin x \tag{22a}$$

$$\dot{X} = -1 - \alpha_0 \sin X \cos x \tag{22b}$$

$$\dot{y} = \frac{\alpha_+ x}{x^2 + y^2} \tag{22c}$$

$$\tag{22d}$$

similar to Eqs. (9) for the dipole, but with a difference in the equation for $y(t)$. Asymptotically (22a,22b) give $x(t) + X(t) = \text{const.}$, which justifies the approximation

$$\dot{y} \approx \frac{\text{const.}}{y^2}, \quad y(t) \sim t^{1/3} \tag{23}$$

Indeed, if r is initially large, Eq. (23) shows that it remains large at long times. We confirmed the validity and verified by direct numerical integration of the vortex equations (12), that the asymptotic behavior of the vortex distance follows a power-law with the exponent 1/3 (see Fig. 7).

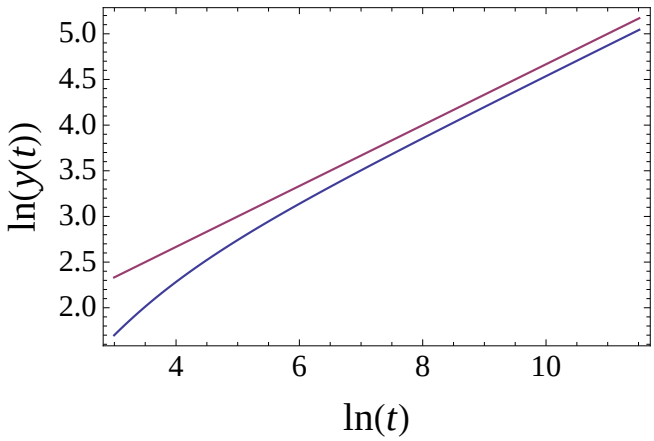

FIG. 7. (Color online) Long-time behavior of the splitting trajectory of Fig. 3 in logarithmic scale. The straight line corresponds to a power-law fit with exponent 1/3.

IV. MERGING OF TWO VORTICES IN THE HASEGAWA-MIMA EQUATION

We consider now the Charney-Hasegawa-Mima equation (2). As mentioned, this equation was introduced in the study of plasma drift waves in a tokamak edge plasma and is known in this context as the Hasegawa-Mima equation; the same equation, referred as the Charney equation, describes Rossby waves geophysical flows. The interest in this equation is that it is able to generate both vortices and waves. Vortex-wave interaction in this

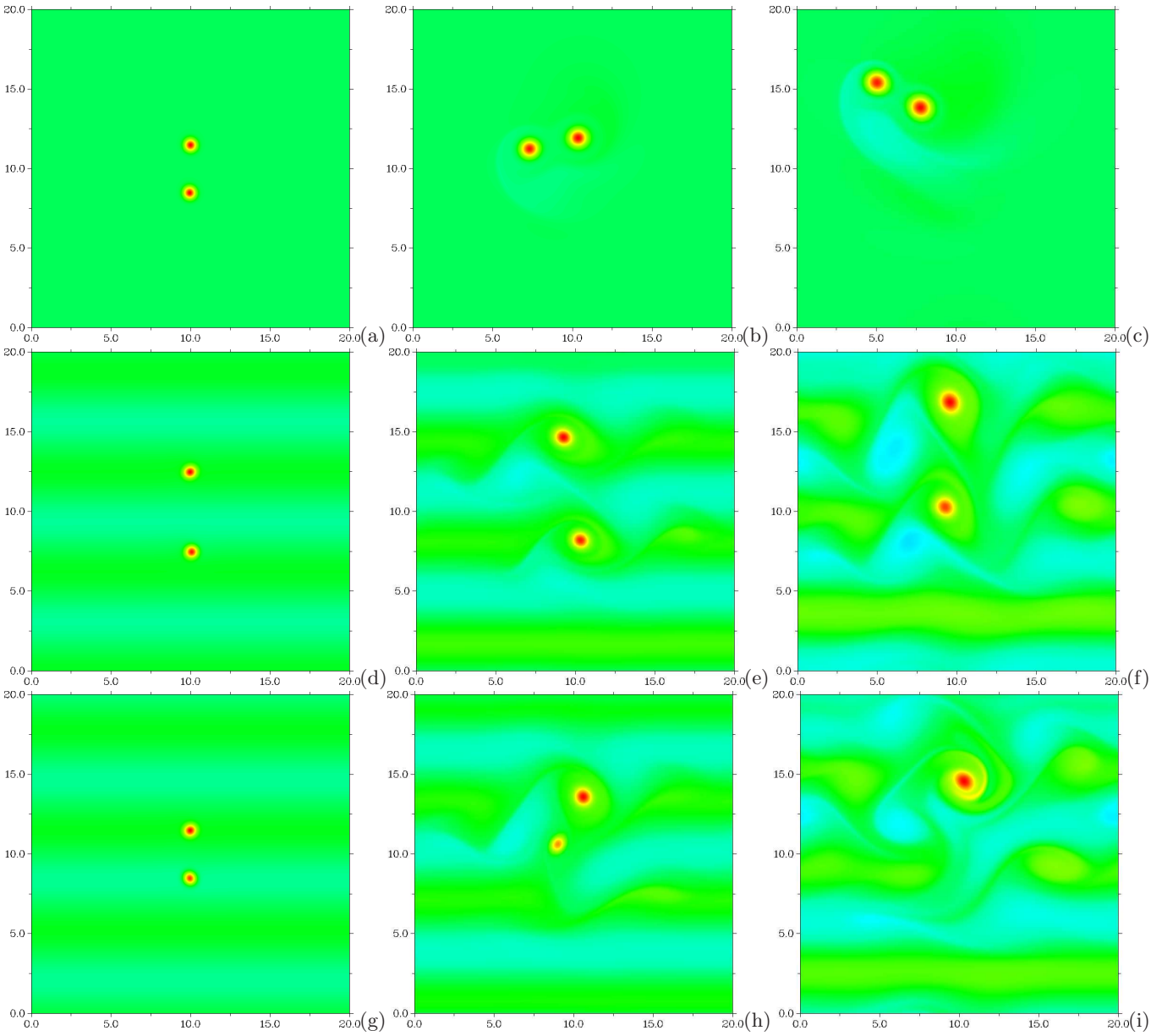

FIG. 8. (Color online) Hasegawa-Mima evolution of two gaussian monopoles. First column (a,d,g), initial state; second column (b,e,h), intermediate state ($t = 7.5\,\rho_s/v_d$); and third column (c,f,i), final state ($t = 15\,\rho_s/v_d$). Row (a-c), the two monopoles distant of $3\,\rho_s$ drift and rotate without merge. Row (d-f), the distance is $5\,\rho_s$ and the wave amplitude is $4\,\rho_s/v_d$; the separation between the two monopoles increases in time. Row (g-i), fusion of two monopoles distant of $3\,\rho_s$ in the presence of a wave (amplitude, $4\,v_d\rho_s$).

system drive a large variety of effects related in particular, to the motion and collisions of localized structures. For instance, a dipole vortex has an oscillatory trajectory when its symmetry axis is inclined with respect to the wave direction of propagation [30], or like-sign vortices (monopoles) may merge under appropriated conditions [14]. We demonstrated theses processes in the context of point vortices. However, in real flows or plasma systems, a vortex has a spatial extension and waves have to obey a specific dispersion relation (3). Moreover, as mentioned in the introduction, the separation of waves and vortices is somewhat arbitrary, their interaction modifies both in such a way that the distinction can be made only within some length scale and time interval. It would then be interesting to analyze how the presence of a wave might influence processes such vortex merging, in the more general framework of the Charney-Hasegawa-Mima equation.

For this purpose we consider two identical vortices; for each vortex we assign at the initial time, a local vorticity

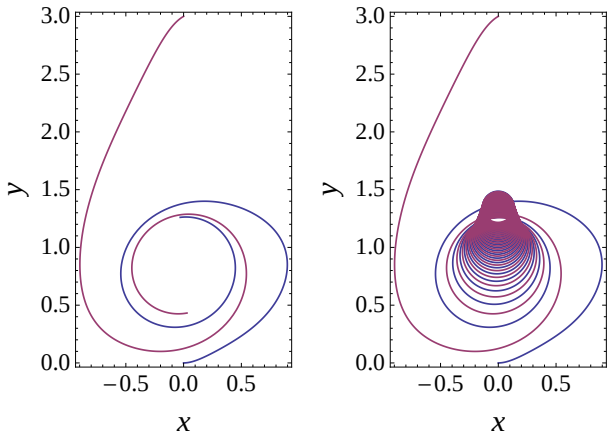

FIG. 9. (Color online) Point vortex trajectories using parameters comparable to the numerical simulation of Fig. 8: $\boldsymbol{r}_1 = (0,0)$, $\boldsymbol{r}_2 = (0,3)$, $\Gamma = 25$, $\Gamma_0 = 4$, and $\omega = 1$. (Left) maximum time 1.015; (Right) maximum time 1.6.

Ω_l in the form of a gaussian,

$$\Omega_l = -\Delta\psi(\boldsymbol{r},0) + \psi(\boldsymbol{r},0)/\rho_s^2 = \frac{b\Gamma_+}{\pi}\exp(-b\,r^2)\,, \quad (24)$$

($\psi(\boldsymbol{r},0)$ is the initial stream function), where b controls the extension of the vortex and Γ_+ it's circulation. Since the waves are naturally appearing in the model we shall not impose an external one, but instead add a wave form to the initial vorticity distribution and see its influence.

In order for vortices to merge, we have found for point vortices that we need a condition of the type $\alpha_0 \sim \alpha_+$, (we notice that the value of ω is not affecting the condition). To simplify things we shall choose as well $|\boldsymbol{k}| = k_y = 1$ (in units of ρ_s). We may then find that the vorticity of a distribution of the type (24), results in $\pi\Gamma_+/b$. Given these facts, the initial condition is chosen as follows

$$\Omega_l = 64\left[\exp(-8r_1^2) + \exp(-8r_2^2)\right] + \varepsilon 4\cos(y-13)\,, \quad (25)$$

where $\varepsilon = 1$ when the wave is present or $\varepsilon = 0$, when it is absent, and $r_{1,2}^2 = (x-x_{1,2})^2 + (y-y_{1,2})^2$, the values of $(x_{1,2}, y_{1,2})$, being adapted to check different cases. It is convenient to introduce the units of length and time in terms of dimensional parameters of the linear dispersion (3), ρ_s and v_d. For the finite range case we put $\rho_s = 1$, and $v_d = 1/2$ such that the frequency of a $k_y = 1/\rho_s$ wave be one. Simulations are made using periodic boundary conditions on a square domain of length $L = 20\,\rho_s$, and the final time corresponds to $t = 15\,\rho_s/v_d$. The numerical code is based on a pseudo-spectral scheme with time stepping a fourth order Runge-Kutta algorithm; the time step is $\delta t = 10^{-3}\,\rho_s/v_d$, the numerical viscosity $\mu = 0.005\,\rho_s v_d$, and the number of spectral modes is 1024^2.

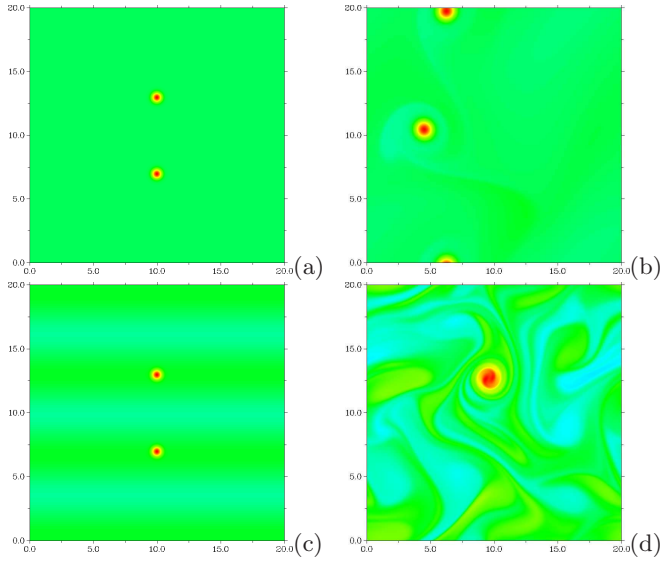

FIG. 10. (Color online) Hasegawa-Mima evolution of two gaussian monopoles in the long range interaction case ($\rho_s = 9.5$, $v_d = 14.5$, and initial distance $6\rho_s$). First row, without wave, (a) initial state ; (b) final state $t = 15\,\rho_s/v_d$ showing the increased separation of the monopoles. Second row, with an initial wave, (c) initial distance $6\rho_s$; (d) final merged state ($t = 15\,\rho_s/v_d$).

We performed a series of simulations changing the initial vortex separation and the presence or not of the wave: (i) we let the two monopoles, separated by a distance of $3\,\rho_s$, evolve freely from the initial positions $(x_1, y_1) = (10,\ 8.5)$, and $(x_2, y_2) = (10,\ 11.5)$, without wave, $\varepsilon = 0$; (ii) we added a wave to the initial state, $\varepsilon = 1$, and choose conditions where our point vortices model predicted splitting (increase of the initial distance, fixed at $5\,\rho_s$ with positions $(x_1, y_1) = (10, 7.5)$, and $(x_2, y_2) = (10,\ 12.5)$), and finally (iii), we chose parameters corresponding to the fusion of the point vortices, with an initial distance of $3\,\rho_s$ and a wave $\varepsilon = 1$ (the initial positions are as in case (i)). Results for the three cases are shown in Fig. 8.

In case (i), shown in Fig. 8a, the monopoles motion results from the superposition of a drift in the y-direction and a rotation around each other; the distance between the vortices remains sensibly constant (it evolves in the viscous time scale). Cases (ii) and (iii), show that when a wave is present, splitting and merging depend on the initial distance (we fixed the other parameters). Figure 8b shows that for far away monopoles, the influence of the initial wave is to reduce significantly the rotation motion and to increase their separation. In contrast, when the initial distance is smaller, the two monopoles tend to merge (case (iii), Fig. 8). The relative position of the monopoles with respect to the wave influences the behavior of their vorticity: the wave possesses its own vorticity which superposes to the monopole one, reinforcing the positive vorticity monopole and weakening the negative vorticity one. This effect, that is not present in the simple

model, although affects the subsequent motion of the vortices, do not change qualitatively the fusion process. We show in Fig. 9 the trajectories of the point vortices that merge under conditions similar to the case (iii) (same vortex circulations, wave amplitude and initial separation). Therefore, we conclude the wave forces the fusion of the vortices, but if the distance between them is too large, the fusion is avoided. This is related to the presence in the vorticity of the Larmor-radius term, which introduces interactions of finite range.

Modifications of the interaction characteristic length, as also studied in the point vortex model where we presented the case $\rho_s \to \infty$, lead to the same distinction between merging or splitting conditions depending on the initial distance (c.f. Fig. 3(b) and Fig. 4(b)). We show in Fig. 10 a simulation with a large $\rho_s = 9.5$ that confirms the influence of the presence of a wave, in the evolution of the two monopoles according to their initial separation. We chose the vortex and wave parameters the same as for the other cases, and $v_d = 14.5$ such that the phase velocity for the $k_y = 1$ is about 0.16; we remark that in the long interaction limit the natural units of length and time are defined by the initial condition. The dispersion relation becomes $\omega = v_d k_y/(\rho_s k)^2$ implying that in this $\rho_s \to \infty$ limit, the combination v_d/ρ_s^2 must be finite for the existence of propagating waves. It is worth noting that the relative position of the initial monopoles with respect to the wave phase of Figs. 10(c), is different from that of case (iii), here the two monopoles are in an positive vorticity wave region; in this case the amplitude of the two monopoles remains nearly the same during their motion, up to the fusion time.

Although we chose to present results on the monopole dynamics in the general case, we note that the point vortex model predicts the oscillations of a dipole in certain directions also observed in dipole systems obeying the Hasegawa-Mima equation [30].

V. CONCLUSIONS

In this paper we introduced a simple model based on the dynamics of point vortices, in order to get an idea on how extended vortices and waves interact in more realistic flows. As a matter of fact, it turned out that this simple model was much richer in the variety of behaviors it could reflect, than what would be expected. Namely, it showed how stable a dipole was, and in opposition how like-circulation vortices could be destroyed or merged by a wave. Comparison of the point vortex plus wave analytical results and the Charney-Hasegawa-Mima simulations, shown that the distinction between localized and extended vorticity is justified by the existence of well separated length and time scales, and is also relevant to determine, for instance, the conditions for vortex merging or splitting.

The results obtained in the case of the point vortex model and confirmed by numerical simulations of a much more complex system, could partially explain how coherent structures can appear by the merging of small structures and then organize themselves into dipoles and monopoles, especially in systems where waves can be present or generated by the dynamics of the structures. We may hope that this simple model, that permits to identify the range of parameters relevant for the vortex-wave interactions, could be a help in the understanding the dynamics of large coherent structures in decaying turbulent flows.

ACKNOWLEDGMENTS

The authors gratefully acknowledge helpful discussions with O. Agullo. We would also like to thank the laboratories PIIM and IRPHÉ, for hospitality and support during the early development of this work.

[1] N. J. Zabusky and J. C. McWilliams, Phys. Fluids **25**, 2175 (1982).
[2] A. Hasegawa, C. G. Maclennan, and Y. Kodama, Phys. Fluids. **22**, 2122 (1979).
[3] V. Zeitlin, *Nonlinear dynamics of rotating shallow water: Methods and advances*, edited by A. C. J. Luo and G. Zaslavsky, Advances in Nonlinear Science and Complexity, Vol. 2 (Elsevier Science, 2007) Chap. Introduction: Fundamentals of rotating shallow water model in the geophysical fluid dynamics perspective, pp. 1–45.
[4] A. Hasegawa and K. Mima, Phys. Rev. Lett. **39**, 205 (1977).
[5] P. H. Diamond, S.-I. Itoh, K. Itoh, and T. S. Hahm, Plasma Physics and Controlled Fusion **47**, R35 (2005).
[6] J. M. Kosterlitz and J. D. Thouless, J. Phys. C: Solid State Phys. **6** (1973).
[7] X. Leoncini, A. Verga, and S. Ruffo, Phys. Rev. E **57**, 6377 (1998).
[8] J. C. McWilliams, J. Fluid Mech. **146**, 21 (1984).
[9] A. Provenzale, Annu. Rev. Fluid Mech. **31**, 55 (1999).
[10] A. Bracco, J. C. McWilliams, A. Provenzale, G. Morante, and J. B. Weiss, Phys. Fluids **12**, 2931 (2000).
[11] F. Dupont, R. I. McLachlan, and V. Zeitlin, Phys. Fluids **10**, 3185 (1998).

[12] S. V. Annibaldi, G. Manfredi, and R. O. Dendy, Phys. Plasmas **9**, 791 (2002).
[13] X. Leoncini, O. Agullo, S. Benkadda, and G. M. Zaslavsky, Phys. Rev. E **72** (2005).
[14] W. Horton, Phys. Reports **192**, 1 (1990).
[15] C. Ferro Fontán and A. Verga, Phys. Rev. E **52**, 6717 (1995).
[16] W. Horton, Rev. Mod. Phys. **71**, 735 (1999).
[17] W. H. Matthaeus, W. T. Stribling, D. Martinez, S. Oughton, and D. Montgomery, Physica D **51**, 531 (1991).
[18] L. Onsager, Nuovo Cimento, Suppl. **6**, 279 (1949).
[19] C. Ferro Fontán and A. Verga, Phys. Rev. E **52**, 6717 (1995).
[20] O. Agullo and A. Verga, Phys. Rev. E **69**, 056318 (2004).
[21] F. Spineanu and M. Vlad, Phys. Plasmas **12**, 112303 (2005).
[22] M. Lessieur, *Turbulence in fluids* (Kluwer Academic, Dordrecht, 1990).
[23] W. Horton and A. Hasegawa, Chaos **4**, 227 (1994).
[24] E. Kim and P. H. Diamond, Phys. Rev. Lett. **88**, 225002 (2002).
[25] M. Kono and W. Horton, Physics of Fluids B: Plasma Physics **3**, 3255 (1991).
[26] C. Marchioro and M. Pulvirenti, *Mathematical theory of uncompressible nonviscous fluids*, Applied mathematical science, Vol. 96 (Springer-Verlag, New York, 1994).
[27] P. G. Saffman, *Vortex Dynamics*, Cambridge Monographs on Mechanics and Applied Mathematics (Cambridge University Press, Cambridge, 1995).
[28] M. Paoletti and T. Solomon, EPL (Europhysics Letters) **69**, 819 (2005).
[29] M. Paoletti and T. Solomon, Phys. Rev. E **72**, 46204 (2005).
[30] M. Makino, K. Kamimura, and T. Taniuty, J. Phys. Soc. Japan **50**, 980 (1981).